haematologica
Journal of the Ferrata Storti Foundation

Prognostic impact of Dmax on baseline FDG-PET/CT in newly diagnosed multiple myeloma

by Léo Raffy, Christèle Etchegaray, Elif Hindie, Olivier Saut, Cyrille Hulin, Anna Schmitt and Charles Mesguich

Received: November 13, 2025.
Accepted: June 3, 2026.

Citation: Léo Raffy, Christèle Etchegaray, Elif Hindie, Olivier Saut, Cyrille Hulin, Anna Schmitt and Charles Mesguich. Prognostic impact of Dmax on baseline FDG-PET/CT in newly diagnosed multiple myeloma.
Haematologica. 2026 June 18. doi: 10.3324/haematol.2025.300090 [Epub ahead of print]

Prognostic impact of Dmax on baseline FDG-PET/CT in newly diagnosed multiple myeloma

Léo Raffy[1], Christèle Etchegaray[2], Elif Hindie[1], Olivier Saut[2], Cyrille Hulin[3], Anna Schmitt[4], Charles Mesguich[1,2].

[1] Department of nuclear medicine, University Hospital of Bordeaux, Bordeaux, France

[2] INRIA, Univ. Bordeaux, CNRS, Bordeaux INP, IMB, UMR 5251, Talence, France

[3] Department of onco-hematology, University Hospital of Bordeaux, Bordeaux, France

[4] Department of onco-hematology, Institut Bergonié, Bordeaux

Corresponding and first author :

Léo Raffy, MD

Department of nuclear medicine, University of Bordeaux, Bordeaux, France

Email: leopyraffy@gmail.com

Short running title : FDG-PET Dmax Prognostic Value in Multiple Myeloma

Word Count (main text) : Approximately 3156 words

Acknowledgments: The authors thank the nuclear medicine technologists and medical physicists of Bordeaux University Hospital and Institut Bergonié for their contribution to image acquisition and data management. The authors are also grateful to the help of INRIA Bordeaux.

Funding : This research did not receive any specific grant from funding agencies in the public, commercial, or not-for-profit sectors.

Data Availability Statement : The datasets generated and analyzed during the current study are available from the corresponding author upon reasonable request.

Conflict of Interest : All the authors declare no competing financial interests and no non-financial conflicts of interest related to this work.

Author Contributions

*LR designed the study, performed PET/CT image analysis, conducted statistical analyses, and drafted the manuscript.

CE and OS developed and supervised the image processing and quantitative analysis pipeline. CH and AS collected clinical data and contributed to patient management.

#CM conceived and supervised the study, conducted statistical analyses, interpreted the data, and critically revised the manuscript for important intellectual content.

EH conceived and supervised the study.

All authors reviewed the manuscript, approved the final version, and agree to be accountable for all aspects of the work.

ABSTRACT

This study aimed to evaluate the prognostic significance of FDG-PET/CT–derived biomarkers, including volumetric and dissemination metrics, in newly diagnosed multiple myeloma (NDMM). A total of 146 NDMM patients who underwent baseline FDG-PET/CT before any treatment between 2014 and 2022 at two institutions were retrospectively analyzed. Metabolic tumor burden was quantified using total metabolic tumor volume (TMTV) and total lesion glycolysis (TLG), while spatial dissemination was assessed by the maximal interlesional distance (Dmax), defined as the greatest three-dimensional Euclidean distance between lesion centroids. Lesions were segmented semi-automatically using LIFEx software with a 41% SUVmax threshold and a minimum SUV of 2.5. Progression-free survival (PFS) and overall survival (OS) were estimated by the Kaplan–Meier method, and optimal cutoffs were determined using maximally selected rank statistics. Among PET-derived parameters, TMTV and Dmax were significantly associated with PFS and OS and retained independent prognostic value after adjustment for clinical and biological prognostic factors. In multivariate analysis performed in separate models due to collinearity, TMTV > 18.6 cm^3 (PFS: HR = 2.17, p = 0.003; OS: HR = 2.23, p = 0.04) and Dmax > 23.2 cm (PFS: HR = 1.89, p = 0.01; OS: HR = 2.69, p = 0.01) remained independent prognostic factors. Dmax represents an independent PET-derived biomarker reflecting spatial disease dissemination in NDMM. The combined evaluation of dissemination and volumetric parameters may improve baseline risk stratification, providing a more comprehensive assessment of disease biology and potentially guiding therapeutic decisions in multiple myeloma.

INTRODUCTION

Multiple myeloma (MM) is the second most common hematologic malignancy (1), characterized by the clonal proliferation of plasma cells within the bone marrow (2). Despite major therapeutic advances, approximately 20% of newly diagnosed multiple myeloma (NDMM) patients still experience poor outcomes (3,4). Identifying robust prognostic biomarkers to guide personalized treatment strategies therefore remains a critical clinical challenge. In current practice, risk stratification mainly relies on the Revised International Staging System (R-ISS) and cytogenetic profiling of bone marrow samples (5). 18F-fluorodeoxyglucose positron emission tomography combined with computed tomography (FDG-PET/CT) is recommended for the initial staging of NDMM while whole-body magnetic resonance imaging is considered an accepted alternative imaging modality for disease staging and prognostic assessment according to current guidelines (6,7). Several studies have demonstrated that specific FDG-PET/CT parameters are associated with poor outcomes in both overall survival (OS) and progression-free survival (PFS). These include a high maximum standardized uptake value (SUVmax) and the detection of a high number of focal lesions (FL), cutoffs varying among the studies (8–10). The prognostic significance of paramedullary disease (PMD) and extramedullary disease (EMD) has also been demonstrated in several works (11,12). Furthermore, quantitative metabolic parameters such as total metabolic tumor volume (TMTV) and total lesion glycolysis (TLG) have also been associated with inferior OS and PFS (13,14). TMTV reflects the total volume of 18F-FDG–avid lesions and hence provides a more complete assessment of tumor burden than previous surrogates such as lactate dehydrogenase levels. However, these conventional PET biomarkers mainly reflect tumor burden and metabolic activity, without accounting for the spatial dissemination of lesions throughout the body. The aim of this study was to evaluate FDG-PET/CT derived features, including volumetric biomarkers and the maximal lesion dissemination distance (Dmax) — defined as the greatest three-dimensional Euclidean distance between the centroids of hypermetabolic lesions — as metrics of tumor burden and spatial dissemination, which may provide complementary information on disease spread and improve prognostic assessment in NDMM patients.

METHODS

Patients

We retrospectively included NDMM patients who underwent pretreatment FDG-PET/CT evaluation between 2014 and 2022 at two medical centers: Bordeaux University Hospital and Institut Bergonié. The inclusion criteria were: 1) diagnosis of MM according to the International Myeloma Working Group (IMWG) criteria; 2) baseline FDG-PET/CT performed. Patients were excluded if they had initiated chemotherapy or autologous stem cell transplantation (ASCT) before FDG-PET/CT evaluation. All patients provided informed consent, and the study was approved by the local ethics committee.

PET/CT image acquisition

FDG-PET/CT scans were acquired using three systems: a GE Discovery 710-16S (GE Healthcare), a Philips Vereos PET/CT (Philips Healthcare), or a GE Discovery IQ (GE Healthcare). Patients fasted for at least 6 hours, avoided glucose-containing infusions, and refrained from physical activity prior to intravenous injection of 18F-FDG (3 MBq/kg). Whole-body images were obtained from the vertex to the feet. CT acquisitions were performed at 120 kV with a 512 × 512 matrix and voxel sizes of 1 × 1 × 2 mm (Vereos and Discovery IQ) or 1 × 1 × 2.5 mm (Discovery 710-16S). PET images were acquired using a 288 × 288 matrix (2 × 2 × 2 mm voxels) for the Vereos, or 256 × 256 (3 × 3 × 3 mm voxels) for the Discovery systems. Reconstruction was performed using either a standard iterative algorithm (3 iterations, 5 subsets, 2 mm Gaussian filter for the Vereos; 2 iterations, 24 subsets, 6.4 mm filter for the Discovery 710-16S) or a block-sequential regularized expectation maximization (BSREM) algorithm for the Discovery IQ. The median blood glucose level before injection was 0.99 g/L (IQR 0.90–1.12), and the median uptake time between injection and imaging was 64 minutes (IQR 60–70).

Visual and semi-quantitative analysis

FDG-PET/CT images were reviewed on a dedicated workstation (Advantage Workstation; GE Healthcare) by an experienced nuclear medicine physician. Visual analysis followed the Italian Myeloma Criteria for PET Use (IMPeTUs) guidelines (15). FL were defined as areas of increased

uptake relative to physiological bone marrow activity, with or without a corresponding lytic lesion on CT, and visible on at least two consecutive slices. Diffuse bone marrow involvement (DBMI) was defined as homogeneous uptake of the axial and proximal appendicular skeleton exceeding hepatic uptake, or as heterogeneous marrow uptake regardless of intensity (16). A visual assessment using the standard 5-point Deauville scale was performed for all FL, EMD lesions, and DBMI. For semi-quantitative evaluation, the SUVmax of DBMI was measured within a 1 cm^3 spherical region of interest placed in the L4 or L5 vertebral body, excluding FL and benign uptake. Whole-body SUVmax (wbSUVmax) was defined as the highest SUVmax among all FL, EMD lesions, and DBMI.

Segmentation and feature extraction

The LIFEx software (version 7.3.0) was used to semi-automatically segment the volumes of interest for each FL and EMD lesion (17). Segmentation was performed using a fixed threshold of 41% of the lesion SUVmax and a minimum absolute SUV of 2.5, with manual adjustments applied when necessary. Volume-based metabolic parameters were subsequently calculated, including the metabolic tumor volume (MTV) and TLG of the hottest FL, as well as the TMTV and whole-body total lesion glycolysis (wbTLG), encompassing all FL and EMD lesions. TLG was defined as the product of SUVmean and MTV. Diffuse bone marrow involvement (DBMI) was excluded from segmentation and was not incorporated into the calculation of TMTV and wbTLG. Once lesion segmentation was completed, Dmax was calculated automatically without additional operator-dependent input as the greatest three-dimensional Euclidean distance between the centroids of all metabolically active lesions identified on FDG-PET/CT. In patients without any FL/EMD lesions, TMTV and Dmax were assigned a value of zero by convention to allow inclusion in survival analyses, reflecting the absence of metabolically active focal disease. An example of visual and volumetric parameters obtained by FDG-PET/CT in a representative patient are reported in Figure 1.

Statistical analysis

PFS was defined as the time from baseline FDG-PET/CT to the first documentation of progressive disease, relapse, or death from any cause, in accordance with the IMWG criteria (18). Follow-up duration

was estimated using the reverse Kaplan-Meier method. Prognostic thresholds for standard FDG-PET/CT parameters were identified using the maximally selected rank statistics method. Survival rates were estimated using the Kaplan-Meier method, and survival curves were compared using the exact log-rank test. Univariate prognostic analyses for PFS and OS were performed using Cox proportional hazards regression. Variables with a two-sided P-value < 0.05 in univariate analyses were subsequently included in multivariate Cox models. Because cytogenetic data required for R-ISS classification were missing in a substantial proportion of patients, ISS stage was used as the primary clinical covariate in multivariable models to preserve statistical power in the full cohort. Additional exploratory analyses incorporating R-ISS were performed in the subset of patients with available cytogenetic data. Because TMTV and Dmax are moderately correlated but reflect distinct biological dimensions (tumor burden versus spatial dissemination), they were evaluated in separate multivariable models adjusted for the same clinical covariates. All statistical analyses were performed using R software (version 4.6.0; R Foundation for Statistical Computing, Vienna, Austria).

RESULTS

Patients

Among the 155 NDMM patients who underwent FDG-PET/CT at our institutions between 2014 and 2022, 146 patients were ultimately enrolled after meeting the inclusion and exclusion criteria (9 patients had received prior therapy before FDG-PET/CT). The median age was 64 years (IQR 54–70). 22 patients presented with high-risk cytogenetic features, defined by the presence of del(17p), t(4;14), or t(14;16) on fluorescence in situ hybridization (FISH) analysis. 70 patients (48%) underwent autologous stem cell transplantation (ASCT). Baseline clinical characteristics and treatment details are summarized in Table 1. Disease patterns and PET-derived volumetric biomarkers are reported in Table 2. Among the 146 patients, 103 (71%) exhibited FL. The median TMTV was 9.9 cm^3 (IQR 0–564.0), and the median Dmax was 12.2 cm (IQR 0–92.2).

Survival analysis

Univariate analysis

After a median follow-up of 64 months (95% CI 42–130 months), 83 of the 146 patients experienced disease relapse. The median PFS was 43 months (95% CI 36–59 months). In univariate Cox proportional hazards analysis, a high wbSUVmax (> 8.8) was significantly associated with shorter PFS (HR = 1.93; 95% CI 1.20–3.11; p = 0.006), as was the presence of EMD (HR = 2.25; 95% CI 1.24–4.08; p = 0.008). The occurrence of ASCT was associated with better PFS (HR = 0.58; 95% CI 0.37–0.89; p = 0.014) and OS (HR = 0.36; 95% CI 0.19–0.67; p = 0.001). Compared with R-ISS 1, R-ISS 2–3 was significantly associated with shorter PFS (HR = 2.25; 95% CI 1.05–4.82; p = 0.037), whereas for OS, the association did not reach statistical significance (HR = 2.56; 95% CI 0.76–8.61; p = 0.13). Among PET-derived quantitative metrics, TMTV and Dmax showed the strongest association with both PFS and OS. High TMTV (> 18.6 cm^3) and high Dmax (> 23.2 cm) were both significantly associated with shorter PFS (TMTV: HR = 2.17; 95% CI 1.40–3.35; p < 0.001; Dmax: HR = 2.12; 95% CI 1.37–3.29; p = 0.001) and shorter OS (TMTV: HR = 2.43; 95% CI 1.33–4.45; p = 0.04; Dmax: HR = 3.38; 95% CI 1.73–6.19; p < 0.001). Among the 146 patients, 71 (49%) exhibited both low TMTV and low Dmax values, 52 (36%) exhibited

both high TMTV and high Dmax values, and 23 (16%) demonstrated discordant profiles. A strong positive correlation was observed between TMTV and Dmax (Spearman's r = 0.77). Factors associated with PFS and OS in univariate analysis are presented in Table 3.

Multivariate analysis

The primary multivariable analyses were performed in the full cohort using established clinical covariates (ISS stage, EMD, and ASCT). In these models, both TMTV and Dmax remained independently associated with PFS and OS. Multivariate Cox regression analyses were performed for both PFS and OS, including variables that were significant in univariate analysis for both endpoints (Table 4). Because of the strong correlation between TMTV and Dmax, they were not included simultaneously in the same multivariate model. Instead, separate models adjusted for the same covariables were constructed to avoid collinearity. A TMTV > 18.6 cm^3 was identified as an independent predictor of shorter PFS (HR = 2.17; 95% CI 1.30–3.64; p = 0.003) and OS (HR = 2.23; 95% CI 1.06–4.70; p = 0.04) (Model 1). Similarly, a Dmax > 23.2 cm independently predicted shorter PFS (HR = 1.89; 95% CI 1.14–3.13; p = 0.01) and OS (HR = 2.69; 95% CI 1.26–5.74; p = 0.01) (Model 2). Both TMTV and Dmax provided additional prognostic stratification within ISS stages 1–2 and stage 3 (Figure 2).

Additional exploratory analyses incorporating R-ISS were performed in the subset of patients with available cytogenetic data (Supplementary Table 1). Because of missing cytogenetic information, these analyses were restricted to a smaller subset of patients, resulting in limited statistical power. In the MTV-adjusted model (n = 53; 30 PFS events), both R-ISS stage III (HR 12.18; 95% CI 4.23–35.04; p < 0.001) and high MTV (HR 5.69; 95% CI 2.13–15.21; p < 0.001) remained independently associated with inferior PFS. Kaplan–Meier curves combining TMTV and R-ISS categories are shown in Supplementary Figure 1. No independent association was observed for OS in this subset. In the Dmax-adjusted model (n = 42; 26 PFS events), R-ISS stage III (HR 11.62; 95% CI 3.50–38.50; p < 0.001) and EMD (HR 3.35; 95% CI 1.12–10.01; p = 0.03) remained significantly associated with PFS. However, the multivariable effect of Dmax could not be reliably estimated due to sparse data and quasi-complete separation, resulting in unstable HR estimates, and was therefore not interpreted. Importantly, the

reduced number of patients and events in these models did not meet the recommended events-per-variable ratio for stable multivariable Cox regression, which likely contributed to the loss of statistical significance for certain imaging parameters. This limitation supports the interpretation that these findings reflect model instability rather than absence of a true prognostic association.

DISCUSSION

To our knowledge, this study is the first to demonstrate the independent prognostic value of Dmax for both PFS and OS in NDMM patients, irrespective of ISS stage, presence of EMD, or receipt of ASCT. Similar observations have been reported in diffuse large B-cell lymphoma (DLBCL), where Dmax has emerged as a major prognostic imaging biomarker (19). Dmax represents a simple and rapid parameter that is less influenced by technical factors than SUV, MTV, or TLG (20). Furthermore, Dmax measurement is highly reproducible and not affected by operator-dependent segmentation, as it is computed automatically (21). Beyond its methodological robustness, Dmax also captures a distinct biological dimension — spatial dissemination — which is increasingly recognized as a key determinant of tumor aggressiveness and therapeutic resistance. Recent genomic and spatial sequencing studies have demonstrated that myeloma evolution frequently involves the coexistence of multiple subclones across distant bone sites, reflecting ongoing intraclonal heterogeneity and spatially restricted evolutionary trajectories (2). Similar to aggressive lymphomas, the CXCL12/CXCR4 axis plays a pivotal role in the homing and retention of plasma cells within the bone marrow microenvironment. Dysregulation of this pathway facilitates tumor cell migration and dissemination (22–24). Overexpression of CXCR4 enhances adhesion, survival, and drug resistance, whereas its downregulation or functional disruption enables plasma cells to escape the marrow niche and colonize distant skeletal or extramedullary sites. Rasche et al. demonstrated that focal lesions often harbor subclones with altered CXCR4-mediated signaling, supporting a model in which spatial dissemination reflects a biologically aggressive phenotype (2). This dissemination phenotype is associated with high-risk clinical features, including extramedullary disease and circulating tumor plasma cells, both of which predict inferior outcomes (25–27). Schinke et al. recently demonstrated that FL located in long bones are associated with inferior outcomes in multiple myeloma (28). This observation is conceptually aligned with our findings, as both highlight spatial disease dissemination. Accordingly, Dmax may serve as an imaging biomarker of these underlying biological processes, quantifying spatial disease spread in a simple and reproducible manner. We also found that TMTV > 18.6 cm^3 was a strong and independent prognostic factor for both PFS and

OS after adjustment for ISS stage, presence of EMD, and ASCT treatment. McDonald et al. reported that a baseline TMTV > 210 cm^3 was associated with inferior outcomes in 192 multiple myeloma patients enrolled in the Total Therapy 3A protocol (29). Similarly, Terao et al. demonstrated that a TMTV > 56.4 cm^3 was independently associated with shorter PFS and OS in a cohort of 185 NDMM patients, even after adjustment for the Revised International Staging System (R-ISS) and high-risk FDG-PET/CT findings (13). The lower TMTV cutoff value identified in our study compared with previous reports may be attributed to differences in patient populations and treatment regimens, as the Little Rock group primarily studied patients eligible for intensive chemotherapy followed by tandem ASCT, potentially mitigating the negative prognostic impact of higher tumor burdens (30). Additionally, variability in segmentation techniques influences TMTV measurements, and inter-operator variability remains a recognized limitation for standardization (30). Manual identification and segmentation of each lesion are often challenging and time-consuming, and artificial intelligence–based methods could assist in addressing these challenges (31). DBMI on FDG-PET/CT has been reported as a prognostic factor at baseline in multiple myeloma (32). However, the accuracy and specificity of FDG-PET/CT for assessing DBMI are limited, as diffuse uptake is highly susceptible to non-tumoral confounders such as anemia, inflammation, growth factor administration, and reactive bone marrow hyperplasia, which are frequent in this patient population (15,33,34). For these reasons, DBMI was excluded from volumetric and dissemination analyses to ensure that PET-derived biomarkers reflected true tumor burden and spatial disease dissemination.

Our study also confirmed that established PET parameters, such as SUVmax and the presence of EMD, retain prognostic value despite major changes in NDMM management and survival outcomes introduced by newer therapies over the past two decades. However, the prognostic significance of these parameters has varied across recent studies. A pooled analysis from two prospective trials reported that wbSUVmax > 7.1 was associated with inferior OS in transplant-eligible MM patients (8), consistent with our finding that only a SUVmax threshold greater than 8.8 reached prognostic significance. Interestingly, in the CASSIOPEIA trial, Alberge et al. found that PMD, rather than EMD, had the strongest prognostic

impact on PFS (35). In our cohort, PMD was not associated with survival outcomes, although this may be limited by the relatively small number of patients presenting with PMD. Moreover, in contrast to earlier landmark studies, we found that the presence of more than three focal lesions was not associated with either PFS or OS. This finding is consistent with more recent cohorts and suggests that contemporary therapeutic approaches may attenuate the prognostic impact of certain traditional PET biomarkers (36).

Several limitations of this study should be acknowledged. First, its retrospective design introduced heterogeneity in patient treatments; however, this reflects real-world clinical practice, unlike prospective trials that often include younger and fitter patients. ASCT was included in multivariate models, as it represents a well-established and independent impact on outcomes. Induction regimen was not included in multivariate models because treatment categories were heterogeneous and unevenly distributed, leading to small subgroup sizes and reduced statistical power, and because regimen choice was strongly correlated with patient fitness and transplant eligibility, potentially compromising model stability and interpretability. Second, cytogenetic data were incomplete, with 42 patients lacking FISH results for high-risk abnormalities (del(17p), t(4;14), and t(14;16)) according to the R-ISS classification (5). High-risk cytogenetic abnormalities were not associated with OS and PFS in this cohort, likely due to incomplete data and limited statistical power. In particular, the absence of statistical significance for high-risk cytogenetics in univariable analysis should be interpreted cautiously, as it likely reflects the limited number of high-risk cases rather than lack of biological relevance. Another limitation relates to clinical risk stratification. Although multivariable models were adjusted for ISS stage, ISS alone may be suboptimal in contemporary cohorts. Incorporation of R-ISS was explored; however, this resulted in a substantial reduction in sample size due to missing cytogenetic data. In this restricted subgroup, the limited number of analyzable patients and outcome events relative to the number of covariates led to model instability and insufficient statistical power for robust multivariable estimation. Analyses incorporating R-ISS should therefore be considered exploratory given the reduced number of evaluable patients and events.

Imaging biomarkers and cytogenetic risk reflect distinct and complementary aspects of disease biology and are not expected to provide overlapping prognostic information. While cytogenetic abnormalities capture intrinsic tumor characteristics from a single bone marrow sampling site, imaging-derived metrics such as Dmax provide a whole-body assessment of spatial disease dissemination, potentially capturing heterogeneity not accessible through localized sampling. Given the marked spatial and genetic heterogeneity observed in NDMM, disease dissemination likely represents a complementary dimension of biological aggressiveness beyond cytogenetic risk profiling. Future prospective multicenter trials with standardized therapeutic approaches are needed to validate these results. In summary, Dmax is a simple and reproducible imaging biomarker of disease dissemination, with independent and complementary prognostic relevance in NDMM.

REFERENCES

1. Siegel RL, Miller KD, Fuchs HE, et al. Cancer statistics, 2021. CA Cancer J Clin. 2021;71(1):7-33.

2. Rasche L, Schinke C, Maura F, et al. The spatio-temporal evolution of multiple myeloma from baseline to relapse-refractory states. Nat Commun. 2022;13(1):4517.

3. Facon T, Kumar SK, Plesner T, et al. Daratumumab, lenalidomide, and dexamethasone versus lenalidomide and dexamethasone alone in newly diagnosed multiple myeloma (MAIA): overall survival results from a randomised, open-label, phase 3 trial. Lancet Oncol. 2021;22(11):1582-1596.

4. Joseph NS, Kaufman JL, Dhodapkar MV, et al. Long-term follow-up results of lenalidomide, bortezomib, and dexamethasone induction therapy and risk-adapted maintenance approach in newly diagnosed multiple myeloma. J Clin Oncol. 2020;38(17):1928-1937.

5. Palumbo A, Avet-Loiseau H, Oliva S, et al. Revised international staging system for multiple myeloma: a report from International Myeloma Working Group. J Clin Oncol. 2015;33(26):2863-2869.

6. Dimopoulos MA, Moreau P, Terpos E, et al. Multiple myeloma: EHA-ESMO Clinical Practice Guidelines for diagnosis, treatment and follow-up. Ann Oncol. 2021;32(3):309-322.

7. Hillengass J, Usmani S, Rajkumar SV, et al. International Myeloma Working Group consensus recommendations on imaging in monoclonal plasma cell disorders. Lancet Oncol. 2019;20(6):e302-e312.

8. Michaud-Robert AV, Zamagni E, Carlier T, et al. Glucose metabolism quantified by SUVmax on baseline FDG-PET/CT predicts survival in newly diagnosed multiple myeloma patients: combined harmonized analysis of two prospective phase III trials. Cancers (Basel). 2020;12(9):2532.

9. Bartel TB, Haessler J, Brown TLY, et al. F18-fluorodeoxyglucose positron emission tomography in the context of other imaging techniques and prognostic factors in multiple myeloma. Blood. 2009;114(10):2068-2076.

10. Zamagni E, Patriarca F, Nanni C, et al. Prognostic relevance of 18F-FDG PET/CT in newly diagnosed multiple myeloma patients treated with up-front autologous transplantation. Blood. 2011;118(23):5989-5995.

11. Moreau P, Attal M, Caillot D, et al. Prospective evaluation of magnetic resonance imaging and 18F-fluorodeoxyglucose positron emission tomography-computed tomography at diagnosis and before maintenance therapy in symptomatic patients with multiple myeloma included in the IFM/DFCI 2009 trial: results of the IMAJEM study. J Clin Oncol. 2017;35(25):2911-2918.

12. Badar T, Srour S, Bashir Q, et al. Predictors of inferior clinical outcome in patients with standard-risk multiple myeloma. Eur J Haematol. 2017;98(3):263-268.

13. Terao T, Machida Y, Hirata K, et al. Prognostic impact of metabolic heterogeneity in patients with newly diagnosed multiple myeloma using 18F-FDG PET/CT. Clin Nucl Med. 2021;46(10):790-796.

14. Fonti R, Larobina M, Del Vecchio S, et al. Metabolic tumor volume assessed by 18F-FDG PET/CT for the prediction of outcome in patients with multiple myeloma. J Nucl Med. 2012;53(12):1829-1835.

15. Nanni C, Versari A, Chauvie S, et al. Interpretation criteria for FDG PET/CT in multiple myeloma (IMPeTUs): final results. Eur J Nucl Med Mol Imaging. 2018;45(5):712-719.

16. Nanni C, Deroose CM, Balogova S, et al. EANM guidelines on the use of 18F-FDG PET/CT in diagnosis, staging, prognostication, therapy assessment, and restaging of plasma cell disorders. Eur J Nucl Med Mol Imaging. 2024;52(1):171-192.

17. Nioche C, Orlhac F, Boughdad S, et al. LIFEx: a freeware for radiomic feature calculation in multimodality imaging to accelerate advances in the characterization of tumor heterogeneity. Cancer Res. 2018;78(16):4786-4789.

18. Kumar S, Paiva B, Anderson KC, et al. International Myeloma Working Group consensus criteria for response and minimal residual disease assessment in multiple myeloma. Lancet Oncol. 2016;17(8):e328-e346.

19. Cottereau AS, Nioche C, Dirand AS, et al. 18F-FDG PET dissemination features in diffuse large B-cell lymphoma are predictive of outcome. J Nucl Med. 2020;61(1):40-45.

20. Fornacon-Wood I, Mistry H, Ackermann CJ, et al. Reliability and prognostic value of radiomic features are highly dependent on choice of feature extraction platform. Eur Radiol. 2020;30(11):6241-6250.

21. Zwanenburg A. Radiomics in nuclear medicine: robustness, reproducibility, standardization, and how to avoid data analysis traps and replication crisis. Eur J Nucl Med Mol Imaging. 2019;46(13):2638-2655.

22. Vandyke K, Zeissig MN, Hewett DR, et al. HIF-2α promotes dissemination of plasma cells in multiple myeloma by regulating CXCL12/CXCR4 and CCR1. Cancer Res. 2017;77(20):5452-5463.

23. Ullah TR. The role of CXCR4 in multiple myeloma: cells' journey from bone marrow to beyond. J Bone Oncol. 2019;17:100253.

24. Rasche L, Chavan SS, Stephens OW, et al. Spatial genomic heterogeneity in multiple myeloma revealed by multi-region sequencing. Nat Commun. 2017;8(1):268.

25. Nowakowski GS, Witzig TE, Dingli D, et al. Circulating plasma cells detected by flow cytometry as a predictor of survival in 302 patients with newly diagnosed multiple myeloma. Blood. 2005;106(7):2276-2279.

26. Gonsalves WI, Rajkumar SV, Gupta V, et al. Quantification of clonal circulating plasma cells in newly diagnosed multiple myeloma: implications for redefining high-risk myeloma. Leukemia. 2014;28(10):2060-2065.

27. Zeissig MN, Zannettino ACW, Vandyke K. Tumour dissemination in multiple myeloma disease progression and relapse: a potential therapeutic target in high-risk myeloma. Cancers (Basel). 2020;12(12):3643.

28. Schinke C, Rasche L, Ashby C, et al. Prognostic impact of focal lesion location and persistence in multiple myeloma: insights from serial PET/DWI imaging. Blood Adv. 2025;9(17):4368-4377.

29. McDonald JE, Kessler MM, Gardner MW, et al. Assessment of total lesion glycolysis by 18F-FDG PET/CT significantly improves prognostic value of GEP and ISS in myeloma. Clin Cancer Res. 2017;23(8):1981-1987.

30. Zirakchian Zadeh M, Ayubcha C, Raynor WY, Werner TJ, Alavi A. A review of different methods used for quantification and assessment of FDG-PET/CT in multiple myeloma. Nucl Med Commun. 2022;43(4):378-386.

31. Capobianco N, Meignan M, Cottereau AS, et al. Deep-learning 18F-FDG uptake classification enables total metabolic tumor volume estimation in diffuse large B-cell lymphoma. J Nucl Med. 2021;62(1):30-36.

32. Li J, Tan H, Xu T, Shi H, Liu P. Bone marrow tracer uptake pattern of PET-CT in multiple myeloma: image interpretation and prognostic value. Ann Hematol. 2021;100(12):2979-2988.

33. Cavo M, Terpos E, Nanni C, et al. Role of 18F-FDG PET/CT in the diagnosis and management of multiple myeloma and other plasma cell disorders: a consensus statement by the International Myeloma Working Group. Lancet Oncol. 2017;18(4):e206-e217.

34. Pilkington P, Lopci E, Adam JA, Kobe C, Goffin K, Herrmann K. FDG-PET/CT variants and pitfalls in haematological malignancies. Semin Nucl Med. 2021;51(6):554-571.

35. Alberge JB, Kraeber-Bodéré F, Jamet B, et al. Molecular signature of 18F-FDG PET biomarkers in newly diagnosed multiple myeloma patients: a genome-wide transcriptome analysis from the CASSIOPET study. J Nucl Med. 2022;63(7):1008-1013.

36. Mesguich C, Hulin C, Latrabe V, et al. Prospective comparison of 18F-FDG PET/CT and whole-body diffusion-weighted MRI in the assessment of multiple myeloma. Ann Hematol. 2020;99(12):2869-2880.

TABLES

TABLE 1. Patients' characteristics at baseline and treatment received.

Characteristic	Value n = 146
Male	85 (58)
Age (y)‡	64 (54-70)
ISS* 1	72 (53)
ISS 2	46 (34)
ISS 3	18 (13)
Hemoglobin (g/dL)‡	12.4 (10.9-13.7)
Platelets (G/L)‡	218 (176-265)
Creatinine (µM/L)‡	78 (62-100)
Calcium (mM/L)‡	2.43 (2.32-2.55)
Albumin (g/dL)‡	38 (34.6-41.0)
LDH (U/L)‡	196 (164-231)
Beta-2-microglobulin (mg/L)‡	2.9 (2.2-4.2)
CRP (mg/L)‡	16 (3.0-36.8)
High-risk cytogenetic†	22 (21%)
ASCT	70 (48%)
Induction therapy	
VRd	52 (36%)
VTd	25 (17%)
MPV	19 (13%)
Rd	10 (7%)
D-VRd	9 (6%)
D-VTd	7 (5%)
Other treatments	24 (16%)

* Missing data in 8 patients; † Missing data in 42 patients (del(17p), t(4;14), or t(14;16))

‡ Data represent median and interquartile range

Unless otherwise noted, data represent number and percentage.

ISS = International Staging System LDH = lactate dehydrogenase; ASCT = autologous stem cell transplant ; CRP = C-reactive protein; VRd = bortezomib lenalidomide dexamethasone; VTd = bortezomib thalidomide dexamethasone; MPV = melphalan prednisone bortezomib; Rd = lenalidomide dexamethasone; D-VRd = daratumumab bortezomib lenalidomide dexamethasone; D-VTd = daratumumab bortezomib thalidomide dexamethasone.

TABLE 2. FDG-PET biomarkers at baseline.

Characteristic	Value n = 146
Presence of FL	103 (70.5%)
> 3 FL	42 (29%)
EMD	14 (9.6%)
PMD	59 (40%)
DBMI	78 (53.4%)
FL SUVmax*	5.0 (0-8.7)
wbSUVmax*	5.7 (4-34.5)
TMTV (cm^3)*	9.9 (0-564.0)
wbTLG (SUV.mL)*	38.0 (0-233.6)
Dmax (cm)*	12.2 (0-92.0)

** Data represent median and interquartile range*

Unless otherwise noted, data represent number and percentage

FL= focal lesion; EMD = extramedullary disease; PMD = paramedullary disease; DBMI = diffuse bone marrow involvement; wbTLG = whole-body total lesion glycolysis.

TABLE 3. Univariate Cox regression analysis of baseline variables for PFS and OS.

Variable	PFS		OS	
	HR (95%CI)	***P***	***HR (95%CI)***	***P***
Age	1.02 (1.00-1.04)	0.07	1.04 (1.01-1.07)	0.012
Male	1.09 (0.69-1.70)	0.7	0.87 (0.84-1.59)	0.7
Increased LDH (> ULN)	1.10 (0.65-1.87)	0.7	2.19 (1.08-4.45)	0.030
3.5 < B2m < 5.5 mg/L	1.80 (1.05-3.08)	0.034	2.56 (1.21-5.43)	0.01
B2m > 5.5 mg/L	4.15 (2.32-7.42)	< 0.001	4.43 (2.04-9.62)	< 0.001
ISS 2-3	2.25 (1.05-4.82)	0.037	3.20 (1.62-6.23)	< 0.001
High-risk cytogenetic	1.62 (0.89-2.94)	0.11	1.42 (0.65-3.15)	0.38
R-ISS 2-3	2.25 (1.05-4.82)	0.037	2.56 (0.76-8.61)	0.13
ASCT	0.58 (0.37-0.89)	0.014	0.36 (0.19-0.67)	0.001
Presence of FL	0.99 (0.61-1.60)	0.98	0.91 (0.85-0.95)	0.12
Number of FL > 3	1.46 (0.92-2.32)	0.11	1.44 (0.76-2.73)	0.26
EMD	2.25 (1.24-4.08)	0.008	2.53 (1.19-5.37)	0.016
PMD	1.50 (0.98-2.32)	0.06	1.64 (0.91-2.97)	0.10
SUVmax (FL/EMD) > 8.8	1.75 (1.10-2.80)	0.019	1.69 (0.90-3.16)	0.09
wbSUVmax > 8.8	1.93 (1.20-3.11)	0.006	1.55 (0.82-2.92)	0.18
TMTV > 18.6 cm^3	2.17 (1.40-3.35)	< 0.001	2.43 (1.33-4.45)	0.004
wbTLG > 75.5 g	1.85 (1.20-2.85)	0.005	2.00 (1.10-3.65)	0.023
Dmax > 23.2 cm	2.12 (1.37-3.29)	0.001	3.28 (1.73-6.19)	< 0.001

LDH = lactate deshydrogenase; B2m = beta-2 microglobulin; ISS = international staging system; ASCT = autologous stem cell transplant; FL = focal lesions; EMD = extramedullary disease; PMD = paramedullary disease; TMTV = total metabolic tumor volume; wbTLG = whole-body tumor lesion glycolysis.

Table 4. Multivariate Cox regression analysis of baseline variables for PFS and OS.

Variable	PFS		OS	
	HR (95%CI)	***P***	***HR (95%CI)***	***P***
Model 1				
TMTV > 18.6 cm^3	2.17 (1.30-3.64)	0.003	2.23 (1.06-4.70)	0.04
EMD	1.60 (0.80-3.21)	0.18	1.77 (0.76-4.15)	0.19
ISS 2	1.99 (1.16-3.39)	0.01	3.49 (1.64-7.42)	0.001
ISS 3	5.84 (2.98-11.4)	< 0.001	5.83 (2.31-14.7)	< 0.001
ASCT	0.52 (0.32-0.85)	0.009	0.33 (0.17-0.66)	0.01
Model 2				
Dmax > 23.2 cm	1.89 (1.14-3.13)	0.01	2.69 (1.26-5.74)	0.01
EMD	1.93 (0.98-3.79)	0.06	1.86 (0.74-4.35)	0.14
ISS 2	1.85 (1.07-3.19)	0.03	3.18 (1.48-6.86)	0.003
ISS 3	5.05 (2.62-9.74)	< 0.001	4.54 (1.83-11.3)	0.001
ASCT	0.55 (0.34-0.91)	0.02	0.48 (0.24-0.94)	0.005

TMTV = total metabolic tumor volume; EMD = extramedullary disease; ISS = international staging system; ASCT = autologous stem cell transplant.

FIGURE LEGENDS

Figure 1. Example of FDG-PET/CT–derived segmentation (TMTV 564 cm^3; Dmax 89 cm). Semi-automatic delineation of focal lesions (FL) and extramedullary disease (EMD) was performed using a 41% SUVmax threshold and SUV >2.5. Dmax corresponds to the largest three-dimensional Euclidean distance between the centroids of the two most distant hypermetabolic lesions.

Figure 2. Prognostic impact of TMTV and Dmax on survival outcomes in NDMM patients.

(A) Kaplan–Meier curves representing PFS according to Dmax > 23.2 cm and ISS stage (1-2 vs 3)

(B) Kaplan–Meier curves representing OS according to Dmax > 23.2 cm and ISS stage (1-2 vs 3)

(C) Kaplan–Meier curves representing PFS according to TMTV > 18.6 cm^3 and ISS stage (1-2 vs 3)

(D) Kaplan–Meier curves representing OS according to TMTV > 18.6 cm^3 and ISS stage (1-2 vs 3)

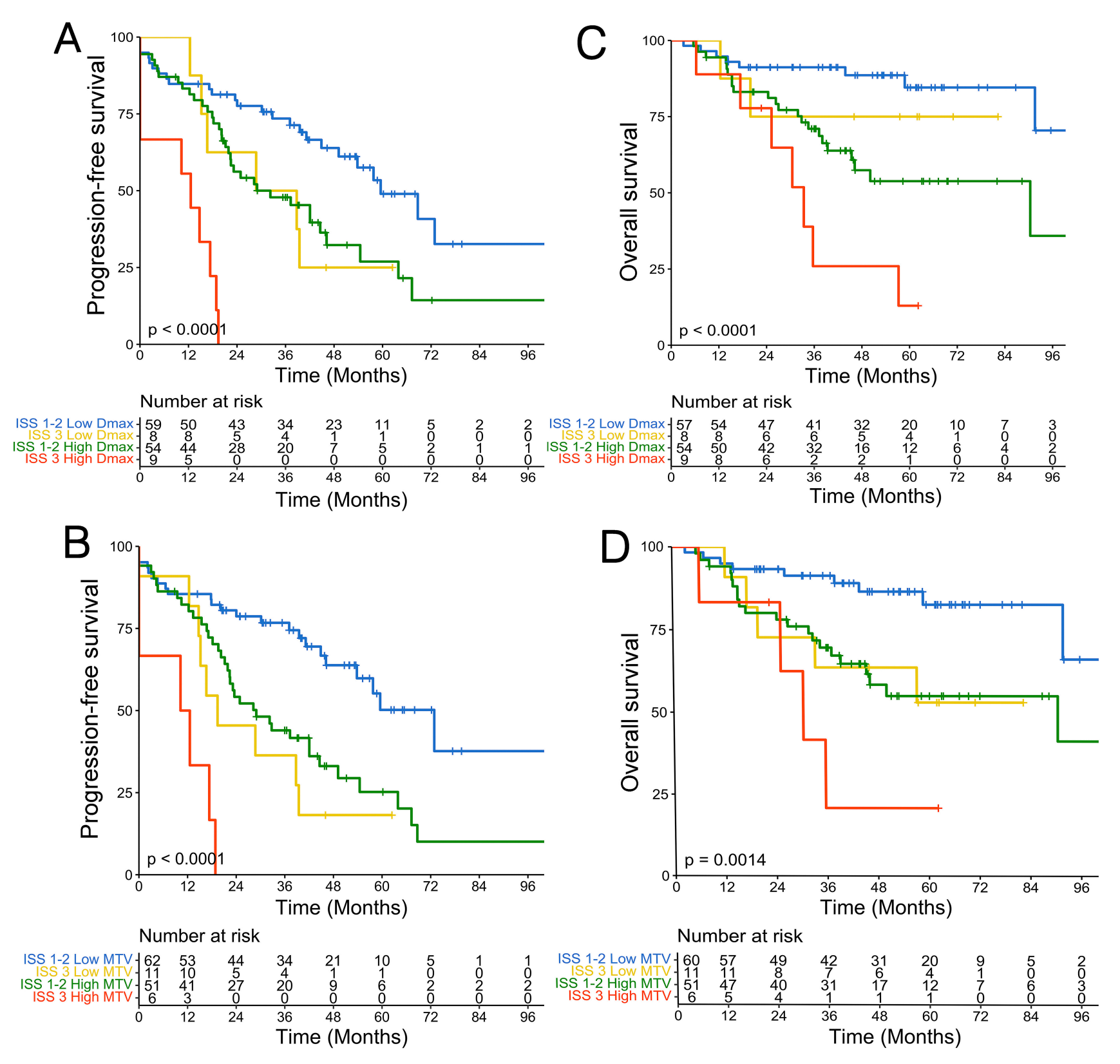
A
Progression-free survival
p < 0.0001
Time (Months)
Number at risk
ISS 1-2 Low Dmax 59 50 43 34 23 11 5 2 2
ISS 3 Low Dmax 8 8 5 4 1 1 0 0 0
ISS 1-2 High Dmax 54 44 28 20 7 5 2 1 1
ISS 3 High Dmax 9 5 0 0 0 0 0 0 0
Time (Months)
C
Overall survival
p < 0.0001
Time (Months)
Number at risk
ISS 1-2 Low Dmax 57 54 47 41 32 20 10 7 3
ISS 3 Low Dmax 8 8 6 6 5 4 1 0 0
ISS 1-2 High Dmax 54 50 42 32 16 12 6 4 2
ISS 3 High Dmax 9 8 6 2 2 1 0 0 0
Time (Months)
B
Progression-free survival
p < 0.0001
Time (Months)
Number at risk
ISS 1-2 Low MTV 62 53 44 34 21 10 5 1 1
ISS 3 Low MTV 11 10 5 4 1 1 0 0 0
ISS 1-2 High MTV 51 41 27 20 9 6 2 2 2
ISS 3 High MTV 6 3 0 0 0 0 0 0 0
Time (Months)
D
Overall survival
p = 0.0014
Time (Months)
Number at risk
ISS 1-2 Low MTV 60 57 49 42 31 20 9 5 2
ISS 3 Low MTV 11 11 8 7 6 4 1 0 0
ISS 1-2 High MTV 51 47 40 31 17 12 7 6 3
ISS 3 High MTV 6 5 4 1 1 1 0 0 0
Time (Months)

Supplementary Table 1. Multivariate Cox regression analysis of baseline variables for PFS and OS including R-ISS.

Variable	PFS		OS	
	HR (95%CI)	***P***	***HR (95%CI)***	***P***
Model 3				
TMTV > 18.6 cm^3	5.69 (2.13-15.21)	<0.001	3.24 (0.89-11.87)	0.076
EMD	2.61 (0.86-7.92)	0.09	7.74 (1.95-30.74)	0.004
ASCT	0.80 (0.36-1.78)	0.058	0.30 (0.10-0.85)	0.024
R-ISS 3	12.18 (4.23-35.04)	<0.001	1.87 (0.62-5.58)	0.26
Model 4				
Dmax > 23.2 cm	Not reliably estimable	/	Not reliably estimable	/
EMD	3.35 (1.12-10.01)	0.03	8.76 (2.31-33.26)	0.001
ASCT	0.97 (0.39-2.38)	0.94	0.32 (0.11-0.94)	0.039
R-ISS 3	11.62 (3.50-38.50)	< 0.001	1.58 (0.52-4.78)	0.042

Supplementary Figure 1. Kaplan–Meier curves representing PFS according to TMTV > 18.6 cm^3 and R-ISS stage (1-2 versus 3)